AGU ADVANCING EARTH AND SPACE SCIENCE

Geophysical Research Letters

RESEARCH LETTER
10.1029/2021GL096765

Properties of Plasmoids Observed in Saturn's Dayside and Nightside Magnetodisc

Y. Xu[1,2], R. L. Guo[3,4], Z. H. Yao[1,2], D. X. Pan[1], W. R. Dunn[5], S.-Y. Ye[6], B. Zhang[7], Y. X. Sun[8], Y. Wei[1], and A. J. Coates[5]

[1]Key Laboratory of Earth and Planetary Physics, Institute of Geology and Geophysics, Chinese Academy of Sciences, Beijing, China, [2]College of Earth and Planetary Sciences, University of Chinese Academy of Sciences, Beijing, China, [3]Laboratory for Planetary and Atmospheric Physics, STAR Institute, Université de Liège, Liège, Belgium, [4]Laboratory of Optical Astronomy and Solar-Terrestrial Environment, Institute of Space Sciences, School of Space Science and Physics, Shandong University, Weihai, Shandong, China, [5]UCL Mullard Space Science Laboratory, Dorking, UK, [6]Department of Earth and Space Sciences, Southern University of Science and Technology (SUSTech), Shenzhen, China, [7]Department of Earth Sciences, The University of Hong Kong, Hong Kong SAR, China, [8]Institute of Space Physics and Applied Technology, School of Earth and Space Sciences, Peking University, Beijing, China

Key Points:

- This study reveals the existence of plasmoids in Saturn's dayside magnetodisc
- A global local time distribution of plasma properties in plasmoid is obtained
- We infer the evolution of plasmoid during rotation from electron density distribution

Supporting Information:

Supporting Information may be found in the online version of this article.

Correspondence to:

Z. H. Yao,
z.yao@ucl.ac.uk

Citation:

Xu, Y., Guo, R. L., Yao, Z. H., Pan, D. X., Dunn, W. R., Ye, S.-Y., et al. (2021). Properties of plasmoids observed in Saturn's dayside and nightside magnetodisc. *Geophysical Research Letters*, *48*, e2021GL096765. https://doi.org/10.1029/2021GL096765

Received 27 OCT 2021
Accepted 20 NOV 2021
Corrected 28 JAN 2022

This article was corrected on 28 JAN 2022. See the end of the full text for details.

Abstract

Plasmoid is a key structure for transferring magnetic flux and plasma in planetary magnetospheres. At Earth, plasmoids are key media which transfer energy and mass in the "Dungey Cycle." For giant planets, plasmoids are primarily generated by the dynamic processes associated with "Vasyliunas cycle." It is generally believed that planetary magnetotails are favorable for producing plasmoids. Nevertheless, recent studies reveal that magnetic field lines could be sufficiently stretched to allow magnetic reconnection in Saturn's dayside magnetodisc. In the study, we report direct observations of plasmoids in Saturn's dayside magnetodisc for the first time. Moreover, we perform a statistical investigation on the global plasmoid electron density distribution. The results show an inverse correlation between the nightside plasmoid electron density and local time, and the maximum plasmoid electron density around prenoon local time on the dayside. These results are consistent with the magnetospheric circulation picture associated with the "Vasyliunas cycle."

Plain Language Summary

Saturn, Jupiter, and our Earth all have global magnetic fields, which have mainly dipole configurations in space environments. These dipole magnetic fields can protect the planets from being directly bombarded by solar wind-charged particles, and thus form a so-called "magnetosphere" that has a stretched tail on the night side and a more dipolar configuration on the dayside. Magnetic reconnection between the interacting regions is the key process which transfers particles and energy. Many magnetic structures are produced in the reconnection region. Plasmoids, fundamental magnetic structures, are key media to transport particles between different regions of a magnetosphere, and to release particles to interplanetary space. Therefore, the characteristics of plasmoid distribution, plasma properties, and formation conditions are pivotal in understanding mass and energy circulations in planetary space. In the present study, we report, for the first time, plasmoids in Saturn's dayside magnetodisc and present their statistical properties. From the statistical distributions, we also infer a potential evolution of plasmoids during planetary rotation, and compare with theoretical models.

1. Introduction

Plasmoids are fundamental elements in transporting magnetic flux and mass at the Earth (Machida et al., 2000), Mercury (DiBraccio et al., 2015), and giant planets (Vogt et al., 2014). In a two-dimensional picture, plasmoids are ideally magnetic loops (also known as magnetic islands), and in the three-dimensional case, they are flux ropes which can be nearly force-free (no plasma pressure gradients and $J \times B = 0$). Flux rope-type plasmoids have enhanced axial magnetic fields and a minimum in plasma density in their core regions while loop-type plasmoids have decreased magnetic field intensity and enhanced plasma density in their cores (e.g., Ieda et al., 1998; Slavin et al., 2003; Zong et al., 2004). Hones (1977) predicted the formation of closed loops of magnetic flux between the near and distant current sheet which he termed "plasmoids," which were observed in the mid-1980s by ISEE 3 (Baker et al., 1987; Hones et al., 1984; Slavin et al., 1989). It is often believed that magnetic reconnection is a key driver for a plasmoid (Slavin et al., 2003). Recent investigations show that magnetic reconnection could take place in the near-Earth (6–10 R_E) magnetotail (Angelopoulos et al., 2008; Lui, 1996). Plasmoids are considered

to be an important consequence of astrophysical and space plasma eruptions, e.g., during solar coronal mass ejections (CME; Vourlidas et al., 2012). The bipolar perturbation in the north-south magnetic component (B_z) in a two-dimensional picture is widely adopted as an identifier of plasmoid events in previous literature (e.g., Ieda et al., 1998; Slavin et al., 2003; Zong et al., 2004). Plasmoids are often accompanied by high-speed plasma flows that are associated with energetic ions and electrons (Slavin et al., 2003). At Earth, plasmoids embedded within high-speed plasma flows move Earthward at 451 km/s and move tailward at 431 km/s (Slavin et al., 2003). Increased electron density and accelerated population are found inside the plasmoid (Chen et al., 2008). The typical duration of a plasmoid is about 2 min (Ieda et al., 1998). In contrast, the time scale for the growth and recovery of Earth substorms is about half an hour (Partamies et al., 2015).

Besides at the Earth, magnetic reconnection and plasmoids are also identified in the magnetopauses and magnetotails of Jupiter and Saturn, and magnetic reconnection plays an important role in driving magnetospheric processes in their space environments (Arridge et al., 2016; Badman et al., 2013; Huddleston et al., 1997; Masters, 2017). Observations of the consequent structures of magnetic reconnection (e.g., plasmoids) can diagnose reconnection processes indirectly. Magnetic reconnection processes can be different between Earth and giant planets. For example, magnetic reconnection in Saturn's magnetotail can last for about 19 hr (Arridge et al., 2016), which is almost twice Saturn's rotation period (~11 hr) and is much longer than the reconnection processes identified in the terrestrial magnetotail. The different features of magnetic reconnection may also result in different characteristics of the associated processes (e.g., plasmoids) between the two planets. The plasmoids at Saturn are often loop-type (Jackman et al., 2011) while at Earth they are more frequently seen as flux ropes (Slavin et al., 2003).

In the terrestrial magnetosphere, solar wind-driven reconnection processes are well described by the Dungey cycle (Dungey, 1961). Magnetopause reconnection opens dayside magnetic fluxes, and transfers them to the nightside via the polar cap region. As more and more magnetic flux is accumulated in the tail, a thin plasma sheet is formed, which is unstable and would trigger magnetic reconnection. For the giant planets, the magnetospheric processes are driven by both solar wind and internal sources which are known as "Vasyliunas cycle" (Vasyliunas, 1983). The internal sources are produced by gas production activity of the moons of giant planets (i.e., Io's volcanic activities for Jupiter and Enceladus water vapor eruptions for Saturn). In the Vasyliunas cycle at Saturn, heavy ions produced near the orbit of Enceladus are picked up by the induced electric field which is generated by the planet's rapid rotation. Thus, these particles exert a strong centrifugal force on the magnetic flux tube, leading to a strong stretching of the magnetic field lines near the magnetic equator. The magnetic field lines are most stretched on the nightside due to the lack of dynamic pressure from the solar wind. Also, the closed flux tubes would lengthen while rotating from noon to dusk (Kivelson & Southwood, 2005; Vasyliunas, 1983). The Vasyliunas cycle predicts that plasmoids form and "pinch off" when field lines stretch down the tail (Vasyliunas, 1983).

Delamere et al. (2015) proposed drizzle-like reconnection in Saturn's magnetodisc which could exist at all local times, including the dayside sectors. Later, Yao et al. (2017) reveal that magnetic reconnection sites may corotate with Saturn, and thus suggest that reconnection sites could exist in all local times within the dayside magnetodisc. Guo et al. (2018) show direct evidence of magnetic reconnection in Saturn's dayside magnetodisc by analyzing high-resolution electron distributions and magnetic field from Cassini data set (Dougherty et al., 2004; Young et al., 2004). Since plasmoid formation, magnetic reconnection, and magnetic dipolarization are closely associated plasma processes in planetary magnetospheres, it is natural to expect plasmoids to exist in Saturn's dayside magnetodisc. The evolution and formation of plasmoids at giant planets are vital in understanding the energy coupling processes (e.g., Delamere et al., 2015; Jackman et al., 2008; Jasinski et al., 2019).

In previous studies, the reconnection-associated plasmoids were only reported on the nightside. In this study, we report for the first time plasmoid in Saturn's dayside magnetodisc. The associated energetic particle features are also investigated. Moreover, we survey the Cassini data set for plasmoids on both dayside and nightside, and infer a globally evolving picture by comparing the properties of events at different local times.

2. Observations

The magnetic field in this study is from the Cassini MAG instrument (Dougherty et al., 2004). Thermal ion and electron measurements are provided by the Cassini-CAPS/IMS/ELS (Young et al., 2004), with an energy range up to 28 keV for electrons and up to 50 keV for ions. Moreover, we utilize energetic particle data from the Low-Energy Magnetospheric Measurements System (LEMMS) and the Ion and Neutral Camera (INCA) of

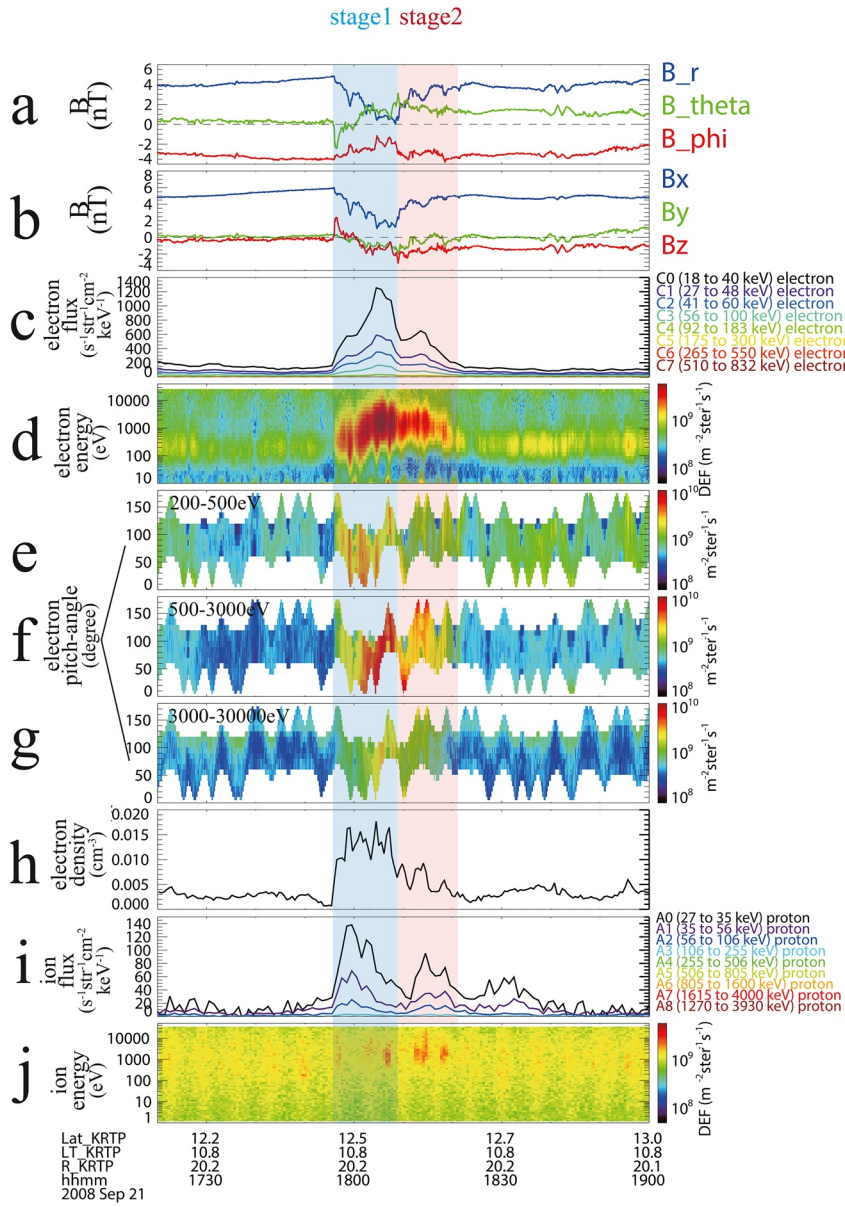

Figure 1. A dayside plasmoid event on 21 September 2008. (a) Three magnetic field components in KRTP coordinates, and (b) in reconnection coordinate. (c) Energetic electron differential flux from MIMI-LEMMS. (d) Energy spectrogram of omnidirectional electron flux from CAPS-ELS. (e–g) Pitch-angle distribution for electrons within energy ranges of 200–500 eV, 500 eV–3 keV, and 3–30 keV. (h) Electron density from CAPS-ELS. (i) Energetic proton differential flux from IMI-LEMMS. (j) Energy spectrogram for omnidirectional ion flux from CAPS-IMS. We divide this event into two stages according to the different magnetic field and plasma properties, which are highlighted in blue and red.

the Magnetosphere Imaging Instrument (MIMI) (Krimigis et al., 2004), which provide coverage of energy range from 18 to 832 keV for electrons, and from 27 to 3,930 keV for ions. Combining the in situ magnetic field and particle data, we obtain pitch-angle information for hot electrons, although the angular coverage is limited due to instrumental issues.

2.1. A Case Study on 21 September 2008

Figure 1 shows observations of a plasmoid event on 21 September 2008, between 17:20 UT and 19:00 UT, during which Cassini was at a radial distance of ~20.2R_S (Saturn's radius, 1 R_s = 60,268 km) from Saturn's center (20.2R_S is in the outer magnetosphere of Saturn). The typical magnetopause standoff distance at Saturn is ~22R_S

(Gombosi et al., 2009) and the local time (LT) is 10.8. Figure 1a shows the magnetic components in Kronographic radial-theta-phi coordinates (a spherical coordinate system in which Z axis represents Saturn's rotation axis, pointing north). Saturn's background field is southward (i.e., positive B_θ) on the magnetic equator (opposite to the Earth case). Figure 1b shows the magnetic field components in the reconnection X-line coordinate system (Arridge et al., 2016; Guo et al., 2018). The magnetic field at Saturn is swept back into a lagging configuration over most local times. The effect of this sweep-back can be generally described by the azimuthal magnetic component. The reconnection coordinate system in Figure 1b could largely eliminate the bend-back effect of the magnetic field lines in the magnetodisc. Figure 1c shows the differential energy fluxes of the electron with energies from 18 to 832 keV measured by the MIMI-LEMMS instrument. The energy spectrogram of omnidirectional hot-electron flux measured by the CAPS-ELS instrument is shown in Figure 1d. Figures 1e–1g show the pitch-angle distribution of electrons in four different energy ranges, from 200 to 500 eV, 500 eV to 3 keV, and 3 to 30 keV (due to the limited field of view of the instrument, the coverage of pitch angles is very poor during the whole period, which is a common situation in the Cassini-CAPS-ELS data set). The electron density obtained by the CAPS-ELS instrument is shown in Figure 1h. Figure 1i shows the differential flux of the energetic ions (mainly protons) in the range of 27 keV-4 MeV from the MIMI-LEMMS instrument. Figure 1j shows the energy spectrogram for omnidirectional ion flux measured by the CAPS-IMS instrument.

As indicated by the bipolar variation of B_θ at ∼18 UT (marked by the colored shadow), a plasmoid event was detected by Cassini in the prenoon sector (at ∼10.8 local time). The magnetic field in the reconnection coordinate system (Figure 1b) shows that B_x is dominant before the perturbation at 17:55 UT, indicating that the spacecraft was located in the outer layer of the current sheet. In Figure 1a, we can see that before 17:55 UT, the three components of the magnetic field are in a rather quiet state. From 17:55 UT, the B_θ component experienced a steep drop (down to −2.5 nT) and a rapid rise to above 0 nT, and then gradually recovered to increase, until it reached a local maximum at 18:09. Six minutes later, B_θ is restored to a relatively quiet state. During the bipolar magnetic variation, the electron and ion spectrograms (Figures 1d and 1j) are characterized by higher than ambient plasma energies (electron in the energy range of 100 eV-10 keV, and ion in the energy range of 1–10 keV). Higher energetic electron and ion fluxes in the period were also clearly seen in Figures 1c and 1i. Based on the variation of B_θ that has a peak at 18:09, we divide the event into two stages, as highlighted in blue and red. In stage 1, the electron pitch-angle distribution is isotropic (as shown in Figures 1e–1g), when sharp increases in electron and ion flux (as shown in Figure 1i) were detected. Compared with this, the electron pitch-angle distribution of stage 2 is field-aligned. The peaks of electron and ion fluxes detected in stage 2 were slightly lower than those in stage 1. During the whole period, the B_r component drops significantly from ∼5 nT to near 0 nT and soon returns to ∼4 nT, indicating that the Cassini spacecraft approached the central region of the current sheet and samples the plasmoid near 18:09 UT. The electron density during this time is significantly higher than that of the ambient environment. Two factors may be responsible: (a) the Cassini spacecraft was close to the center of the current sheet and (b) the plasmoid structure is featured with higher plasma density. The duration from the minimal to the maximal value of B_θ lasted 15 min, which was adopted as the duration of the plasmoid in Jackman et al. (2011) (The average duration of 34 plasmoids was 8 min in Jackman et al., 2011)

2.2. A Statistical Investigation of Plasmoid Events

To perform a statistical investigation, we surveyed the Cassini data set from 2005 to 2010. The negative B_θ component is usually considered as an identifier of plasmoids. In the selection of events, we require B_θ to reach a certain negative value. Furthermore, plasmoid events are often featured by a sharp drop of the B_θ component, thus dB_θ/dt is used to restrict our event selection. Considering the complexity of magnetic perturbations in the magnetosheath region that may affect the analysis of plasmoid features, we require a relatively quiet background of magnetic field prior to the selection of plasmoid events. The quiet background is defined by a small standard deviation of the B_θ component of the background magnetic field. The plasma temperature is an additional parameter used to exclude the influence of the magnetosheath region. Considering the great influence and disturbance caused by cold plasma in the inner magnetosphere, we only focus on the events beyond 15 R_s, where the hot plasma dominates. Based on the above considerations, we determine the selection criteria of the plasmoid starting time as below.

1. dB_θ/dt has a negative growth of at least −0.3 nT/min at the event. (We use magnetic field data with 1-min accuracy, so this condition is equivalent to the negative growth of −0.3 nT for ΔB_θ in 1 min.)

2. The minimum value of B_θ within 3 min after the beginning is <-0.5 nT
3. The standard deviation of B_θ from 25 to 10 min before the event is <1.5 nT
4. The location of each event is required to be >15 R_s away from Saturn. (In order to study the concentration properties of Saturn in the noon sector, the definition of the dayside event in this paper is 8–16 hr local time, and the rest is called the nightside.)
5. The maximum electron temperature within 5 min before and after the event beginning is not <90 eV

We define the start time of a plasmoid event as the time when dB_θ/dt first reaches -0.3 nT. Also, the end time is selected when B_θ reaches the first local maximum value (defined as the maximum value within 5 min before and after) which is larger than 0 after recovering from the negative value. It should be noted that the magnetopause is a boundary caused by the continuous interaction between the magnetosheath and the magnetosphere, so that the perturbations of magnetic field and particles are persistent. To avoid potential confusion, we do not select the events in the magnetopause boundary layer in this study.

We eventually identified 111 plasmoid events (60 on the dayside and 51 on the nightside) from 2005 to 2010. Magnetic perturbations due to Titan flybys are excluded in this study. A full list of the events is shown in Table S1. It is noteworthy that the automatedly identified events in this study are substantially different from the list based on eye-identification in previous literature (Jackman et al., 2014). As a reference, we identified 27 events in nightside magnetosphere from the 2006 data set, 12 of which are also included in Jackman et al. (2014). To our experience, 12/27 is a quite reasonable number in such a comparison between two totally different methodologies. A superposed epoch analysis for the Cassini magnetic field and electron density is shown in Figure S3 in Supporting Information S1. The results show that plasmoids at Saturn are often loop-like, with little or no axial core magnetic field, which is consistent with Jackman et al. (2011). As shown in Figures S4 and S5 in Supporting Information S1, both the planetward and outward propagating events can show statistical bipolar variations as previously reported for Earth plasmoids (Slavin et al., 2003). More representative examples of the dayside and nightside events are presented in Figures S8–S12 in Supporting Information S1. To ensure that the electron density is sampled near the center of the current sheet where the density can better characterize a plasmoid, we calculate the average of the electron density for the part of the plasmoid event where |Br| is smaller than 2.5 nT.

Panels a and b of Figure 2 show the global distribution of electron density. The trajectory of the spacecraft is also overlayed on the diagram. The magnetopause position (black curve) is based on the A60 model (Kanani et al., 2010), with solar wind dynamic pressure taken to be 0.006 nPa. We shall bear in mind that the events were produced under varied dynamic pressure, so that it would be meaningless in physics to fit one magnetopause location for all events. All events are well inside this magnetopause, perhaps suggesting that 0.006 nPa is a lower boundary of the solar wind dynamic pressure when these events were produced. Panel c shows the distribution of the ratio of the dayside and nightside plasmoid electron density to the background density (the background electron density is defined as the average electron density from 25 to 10 min ahead of the event). On the dayside, ~80% of the events were located at low latitudes (<30° latitude). While on the nightside, all events were located below 10° latitude (most of Cassini's orbits were at low latitudes [<30°]). We can see in Figure 2a that plasmoid events on the dayside are highly concentrated at local times between 10 LT and 14 LT (this may be related to the orbital distribution of Cassini), and a bunch of high electron density events appear at ~11 LT. At other local times, the electron density is generally low. In the nightside (Figure 2b), the plasmoid events are concentrated in three local times (~21 LT, ~1 LT, ~5 LT). We can qualitatively see an inverse correlation of electron density with radial distance and local time on the nightside. We note that the plasmoid events are not equally distributed on all orbits. This is probably because the different orbits were during different solar wind conditions, which may strongly influence the occurrence of plasmoids. For example, in September 2006, 14 plasmoid events on the nightside are identified successively. For the dayside, the distribution of the plasmoid events is rather scattered. If the events are considered to be observed by a separation of at least 7 days as irrelevant groups, then there are at least 25 groups of dayside events. The occurrence rate of plasmoids in this study is calculated to be 0.4007% (in 21 different orbits).

Among the 111 plasmoid events, we identified 82 loop-like plasmoids (accounting for 73.8%), which indicates that the plasmoids at Saturn are more usually loop-type plasmoids, and is consistent with the findings of Jackman et al. (2011). Panel c of Figure 2 shows the global distribution of the ratio of electron density to the background density of plasmoid events. It is obvious that the electron density for the majority of the events is higher than the

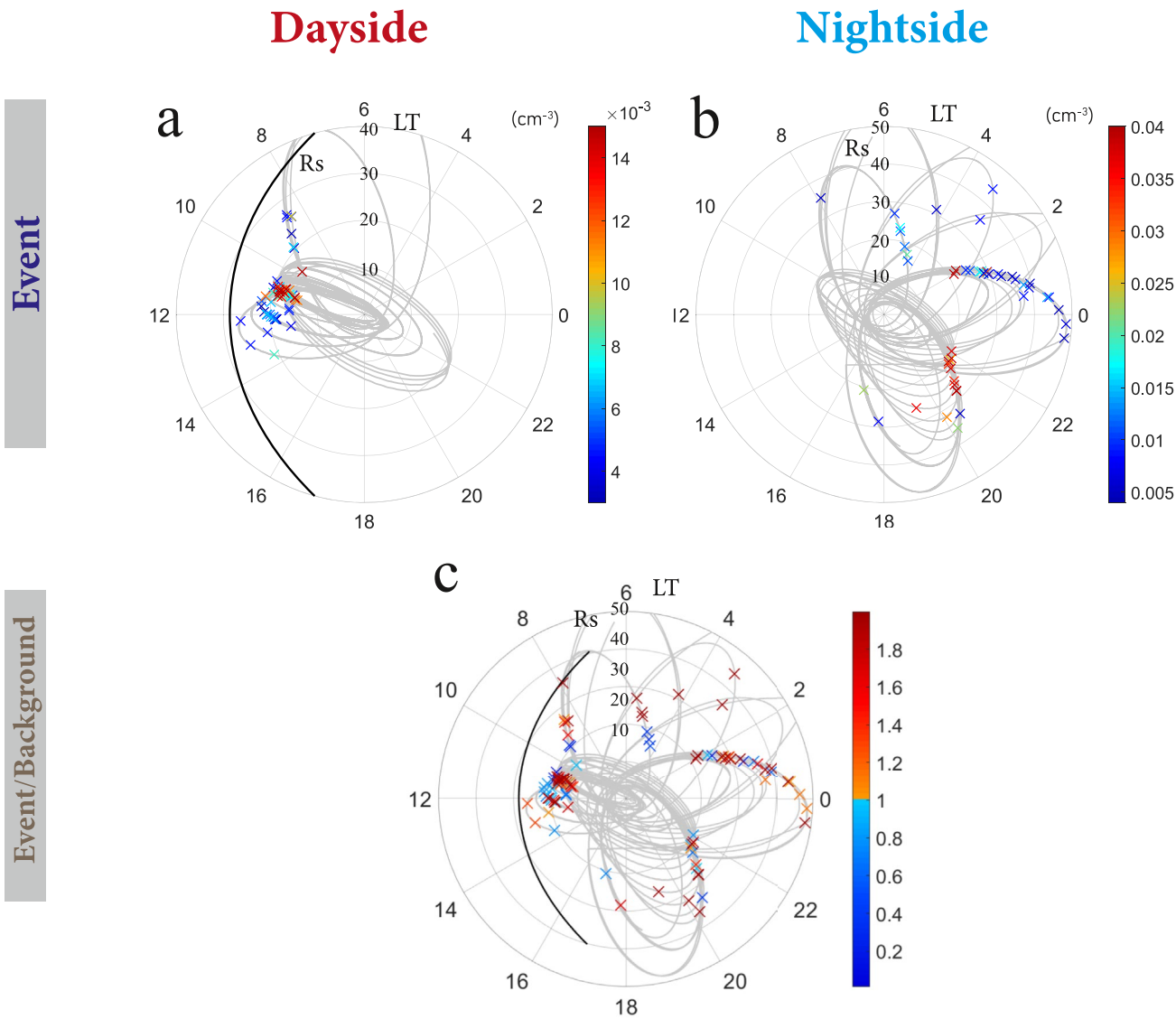

Figure 2. The distribution of plasmoid electron density. Panels a and b show the global distribution of the dayside and nightside electron density respectively. Panel c below shows the ratio of the dayside and nightside plasmoid electron density to the background density. Magnetopause location is plotted by the black curve. The trajectory of the spacecraft is also superimposed on the diagram.

background density. 69/111 events show higher density than their background, in which 33/60 events were on the dayside and 36/51 events were on the nightside, which supports the idea that loop-like plasmoids are more common at Saturn (Jackman et al., 2011).

Figure 3a shows the distribution of electron density at different local times on the dayside, where the red dots represent the plasmoid events at $R < 20\ R_s$, and the blue dots represent the plasmoid events at $R > 20\ R_s$. The electron density has a significant peak at LT ~ 11 when $R < 20\ R_s$. It can be clearly seen from Figure 3a that most of the events (7 of 8 events) with electron density greater than 0.015 (cm^{-3}) are concentrated in the 11 LT region, including most high-density events. The median numbers for two selected sectors, 10:30–11:30 LT and 11:30–12:30 LT, are 0.01028 (cm^{-3}) and 0.00499 (cm^{-3}) shown by the blue squares. We note that Delamere et al. (2015) also find that the peak occurrence of drizzle-like reconnection events is at ~11 LT, which is probably related to the electron density peak of plasmoids in this study. Figure 3b shows the inverse correlation between the electron density on the dayside and the radial distance in the X-Y plane.

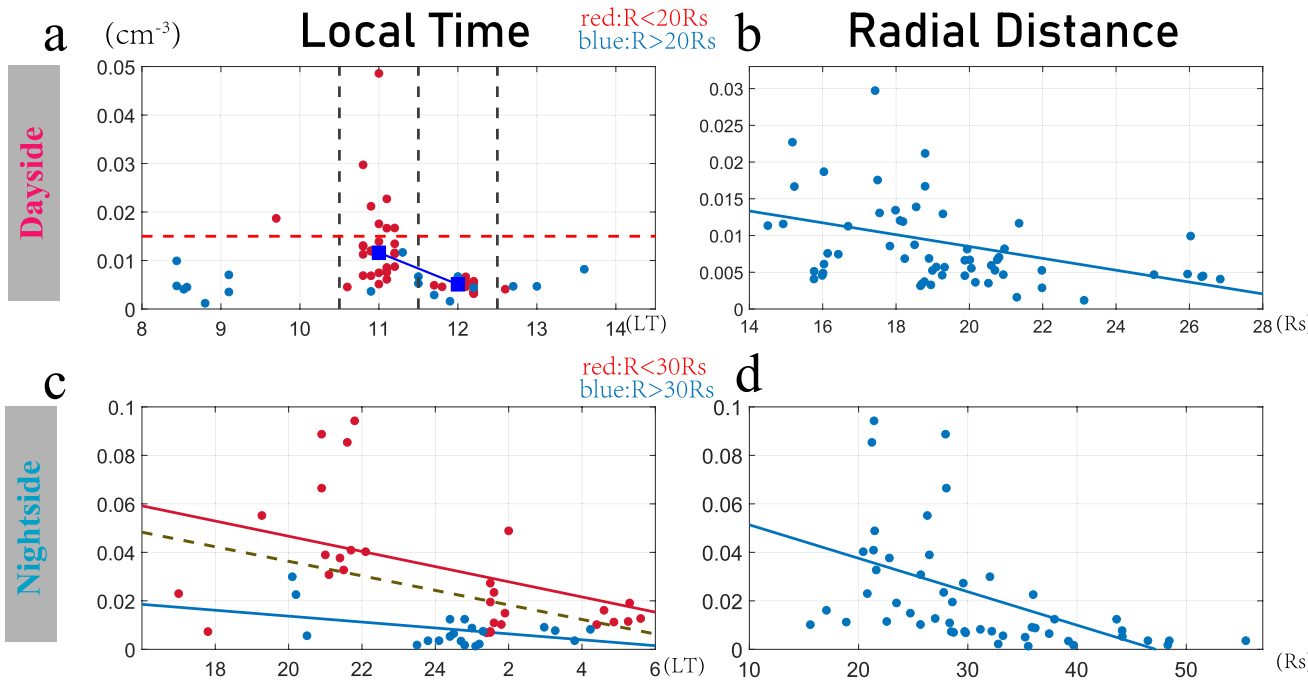

Figure 3. Plasmoid electron density statistical results. (a) The distribution of electron density at different local times in dayside sectors. (b) The distribution of the electron density at different radial distances in dayside sectors. The fitting equation is $y = -0.000806x + 0.0246$, $R^2 = 0.0989$. (c) The distribution of electron density at different local times of nightside. The equation of the red fitting line is $y = -0.00271x + 0.0952$, correlation coefficient $R^2 = 0.176$; the blue line fitting equation is $y = -0.00127x + 0.0397$, $R^2 = 0.260$; the yellow line equation is $y = -0.00265x + 0.0855$, $R^2 = 0.166$; the blue line fitting equation is $y = -0.00168x + 0.0496$, $R^2 = 0.302$. (d) The distribution of the electron density at different radial distances of nightside. The fitting equation is $y = -0.00138x + 0.0652$, $R^2 = 0.229$.

Figure 3c shows the electron density distribution at different local times for nightside sectors, where the red dots represent the plasmoid events of $R < 30\ R_s$ and the blue dots represent the plasmoid events of $R > 30\ R_s$. We find an inverse correlation between the electron density and local time from the dusk-side to the dawn-side. We fitted data when $R < 30\ R_s$, $R > 30\ R_s$ and all events, respectively. The results are clear: from the dusk-side to the dawn-side via midnight, the electron density of plasmoids decreased gradually. The results are consistent with the picture of "Vasyliunas cycle," during which the magnetic flux tube expands radially during the cycle on the nightside, resulting in a significant decrease of its electron density. Similar to Figure 3b, Figure 3d shows the inverse correlation between the electron density on the nightside and the radial distance.

3. Discussion and Conclusion

At giant planets like Saturn and Jupiter, whose magnetospheres rapidly rotate, the mass circulation is dominated by the Vasyliunas cycle (Vasyliunas, 1983). Moreover, reconnection processes which cause the formation of plasmoids are suggested to be small-scale and "drizzle-like" (Delamere et al., 2015; Guo et al., 2019), meaning that plasmoids may be generated at all local times. At different local times, plasmoids show different properties constrained by different conditions. At near-noon local times, the flux tubes are compressed to have a minimum volume. From the dusk-side to the dawn-side, a flux tube would gradually expand. In adiabatic conditions, flux tube expansion would lead to a decrease of electron density, thus we expect a continuous decrease of electron density from the dusk-side to the dawn-side, and the maximum of electron density near noon.

Figure 4 is a cartoon to illustrate the evolution of plasmoids and flux tubes based on the statistical results that are consistent with the expectation from the Vasyliunas cycle. As an alternative explanation, the change in electron density could also be caused by solar wind compression on Saturn's dayside magnetosphere. The solar wind compression is expected to be maximum in the subsolar region, which may lead to an increased electron density. It is also possible that the two effects (i.e., Vasyliunas cycle and the solar wind compression) work together.

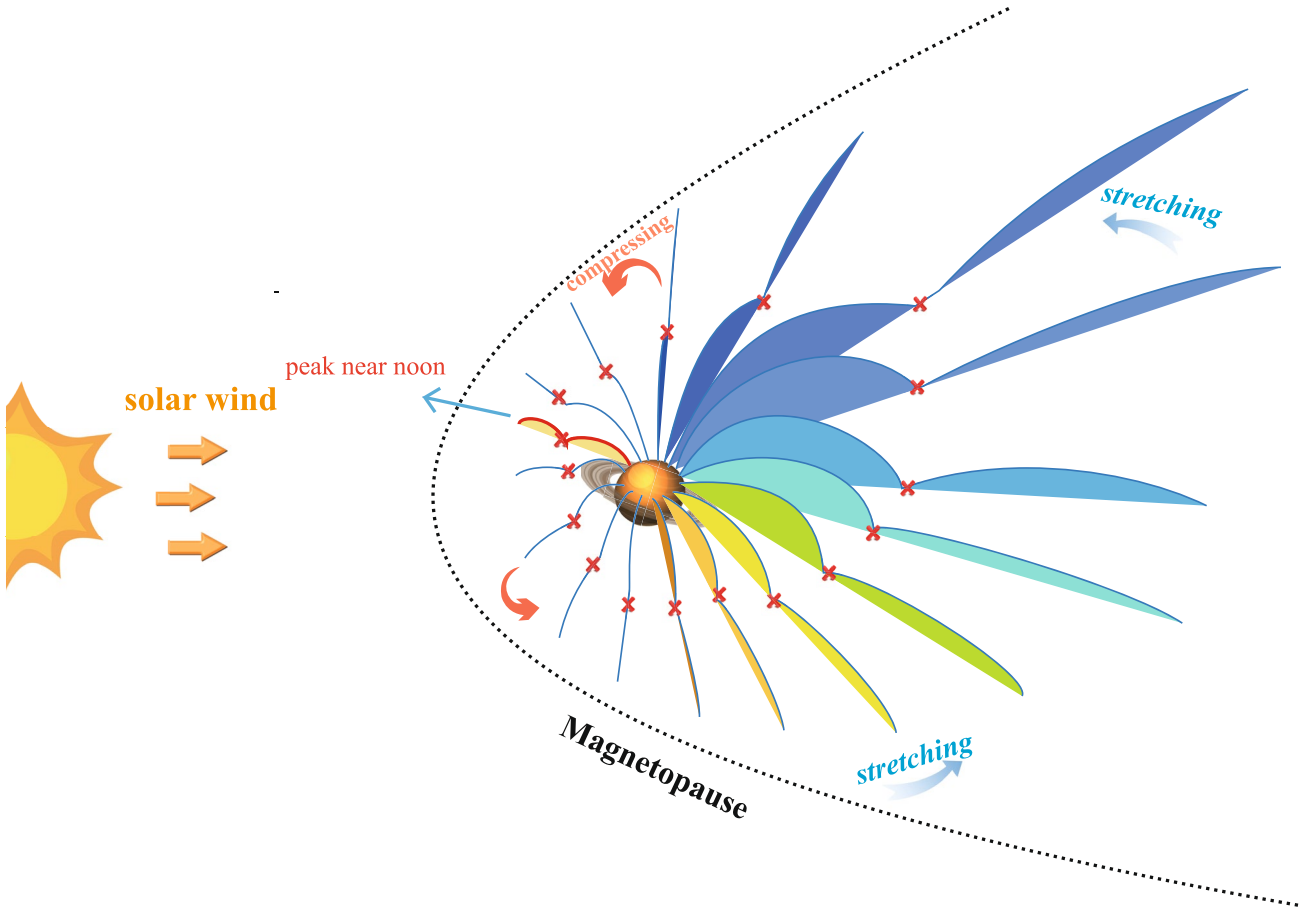

Figure 4. Physical images of the "Vasyliunas cycle" in the magnetosphere of Saturn. The filled color indicates the relative electron density. On the dayside, a peak of electron density is observed near noon.

Data Availability Statement

The Cassini data presented in this study are available at https://pds-ppi.igpp.ucla.edu/search/?t=Saturn&sc=Cassini&facet=SPACECRAFT_NAME&depth=1, from the MAG, CAPS, and MIMI instruments.

Acknowledgments
This work was supported by the Strategic Priority Research Program of Chinese Academy of Sciences, Grant No. XDB 41000000, the National Science Foundation of China (Grant 42074211), and the Key Research Program of the Institute of Geology and Geophysics CAS (Grant IGGCAS-201904). AJC and WD acknowledge support from UCL-MSSL solar system consolidated Grant ST/S000240/1 from STFC, UK. B.Z. was supported by the General Research Fund (17300719 and 17308520) and the Excellent Young Scientists Fund Hong Kong and Macau of the National Natural

References

Angelopoulos, V., McFadden, J. P., Larson, D., Carlson, C. W., Mende, S. B., Frey, H., et al. (2008). Tail reconnection triggering substorm onset. *Science*, *321*(5891), 931–935. https://doi.org/10.1126/science.1160495

Arridge, C. S., Eastwood, J. P., Jackman, C. M., Poh, G. K., Slavin, J. A., Thomsen, M. F., et al. (2016). Cassini in situ observations of long-duration magnetic reconnection in Saturn's magnetotail. *Nature Physics*, *12*(3), 268–271. https://doi.org/10.1038/nphys3565

Badman, S. V., Masters, A., Hasegawa, H., Fujimoto, M., Radioti, A., Grodent, D., et al. (2013). Bursty magnetic reconnection at Saturn's magnetopause. *Geophysical Research Letters*, *40*, 1027–1031. https://doi.org/10.1002/grl.50199

Baker, D., Anderson, R., Zwickl, R., & Slavin, J. J. J. (1987). Average plasma and magnetic field variations in the distant magnetotail associated with near-Earth substorm effects. *Journal of Geophysical Research*, *92*(A1), 71–81. https://doi.org/10.1029/ja092ia01p00071

Chen, L.-J., Bhattacharjee, A., Puhl-Quinn, P. A., Yang, H., Bessho, N., Imada, S., et al. (2008). Observation of energetic electrons within magnetic islands. *Nature Physics*, *4*(1), 19–23. https://doi.org/10.1038/nphys777

Delamere, P. A., Otto, A., Ma, X., Bagenal, F., & Wilson, R. J. (2015). Magnetic flux circulation in the rotationally driven giant magnetospheres. *Journal of Geophysical Research: Space Physics*, *120*, 4229–4245. https://doi.org/10.1002/2015JA021036

DiBraccio, G. A., Slavin, J. A., Imber, S. M., Gershman, D. J., Raines, J. M., Jackman, C. M., et al. (2015). MESSENGER observations of flux ropes in Mercury's magnetotail. *Planetary and Space Science*, *115*, 77–89. https://doi.org/10.1016/j.pss.2014.12.016

Science Foundation of China (41922060). The authors wish to thank the International Space Science Institute in Beijing (ISSI-BJ) for supporting and hosting the meetings of the International Team on "The morphology of auroras at Earth and giant planets: characteristics and their magnetospheric implications," during which the discussions leading/contributing to this publication were held.

Dougherty, M., Kellock, S., Southwood, D., Balogh, A., Smith, E., Tsurutani, B., et al. (2004). The Cassini magnetic field investigation. In C. T. Russell (Ed.), *The Cassini-Huygens Mission* (pp. 331–383). Springer. https://doi.org/10.1007/978-1-4020-2774-1_4

Dungey, J. W. (1961). Interplanetary magnetic field and the auroral zones. *Physical Review Letters*, *6*(2), 47–48. https://doi.org/10.1103/PhysRevLett.6.47

Gombosi, T. I., Armstrong, T. P., Arridge, C. S., Khurana, K. K., Krimigis, S. M., Krupp, N., et al. (2009). Saturn's magnetospheric configuration. In *Saturn from Cassini-Huygens* (pp. 203–255). Springer. https://doi.org/10.1007/978-1-4020-9217-6_9

Guo, R., Yao, Z., Sergis, N., Wei, Y., Xu, X., Coates, A., et al. (2019). Long-standing small-scale reconnection processes at Saturn revealed by Cassini. *ApJL*, *884*(1), L14. https://doi.org/10.3847/2041-8213/ab4429

Guo, R. L., Yao, Z. H., Wei, Y., Ray, L. C., Rae, I. J., Arridge, C. S., et al. (2018). Rotationally driven magnetic reconnection in Saturn's dayside. *Nature Astronomy*, *2*(8), 640–645. https://doi.org/10.1038/s41550-018-0461-9

Hones, E. W. (1977). Substorm processes in the magnetotail: Comments on 'On hot tenuous plasmas, fireballs, and boundary layers in the earth's magnetotail'by LA Frank, KL Ackerson, and RP Lepping. *Journal of Geophysical Research*, *82*(35), 5633–5640. https://doi.org/10.1029/ja082i035p05633

Hones, E. W., Jr, Baker, D., Bame, S., Feldman, W., Gosling, J., McComas, D., et al. (1984). Structure of the magnetotail at 220 RE and its response to geomagnetic activity. *Geophysical Research Letters*, *11*(1), 5–7. https://doi.org/10.1029/gl011i001p00005

Huddleston, D. E., Russell, C. T., Le, G., & Szabo, A. (1997). Magnetopause structure and the role of reconnection at the outer planets. *Journal of Geophysical Research*, *102*(A11), 24289–24302. https://doi.org/10.1029/97JA02416

Ieda, A., Machida, S., Mukai, T., Saito, Y., Yamamoto, T., Nishida, A., et al. (1998). Statistical analysis of the plasmoid evolution with Geotail observations. *Journal of Geophysical Research*, *103*(A3), 4453–4465. https://doi.org/10.1029/97JA03240

Jackman, C., Arridge, C., Krupp, N., Bunce, E., Mitchell, D., McAndrews, H., et al. (2008). A multi-instrument view of tail reconnection at Saturn. *Journal of Geophysical Research*, *113*(A11). https://doi.org/10.1029/2008ja013592

Jackman, C. M., Slavin, J. A., & Cowley, S. W. H. (2011). Cassini observations of plasmoid structure and dynamics: Implications for the role of magnetic reconnection in magnetospheric circulation at Saturn. *Journal of Geophysical Research*, *116*, A10212. https://doi.org/10.1029/2011JA016682

Jackman, C. M., Slavin, J. A., Kivelson, M. G., Southwood, D. J., Achilleos, N., Thomsen, M. F., et al. (2014). Saturn's dynamic magnetotail: A comprehensive magnetic field and plasma survey of plasmoids and traveling compression regions and their role in global magnetospheric dynamics. *Journal of Geophysical Research: Space Physics*, *119*, 5465–5494. https://doi.org/10.1002/2013JA019388

Jasinski, J. M., Arridge, C. S., Bader, A., Smith, A. W., Felici, M., Kinrade, J., et al. (2019). Saturn's open-closed field line boundary: A Cassini electron survey at Saturn's magnetosphere. *Journal of Geophysical Research: Space Physics*, *124*, 10018–10035. https://doi.org/10.1029/2019JA027090

Kanani, S., Arridge, C. S., Jones, G., Fazakerley, A., McAndrews, H., Sergis, N., et al. (2010). A new form of Saturn's magnetopause using a dynamic pressure balance model, based on in situ, multi-instrument Cassini measurements. *Journal of Geophysical Research*, *115*, A06207. https://doi.org/10.1029/2009JA014262

Kivelson, M. G., & Southwood, D. J. (2005). Dynamical consequences of two modes of centrifugal instability in Jupiter's outer magnetosphere. *Journal of Geophysical Research*, *110*, A12209. https://doi.org/10.1029/2005JA011176

Krimigis, S., Mitchell, D., Hamilton, D., Livi, S., Dandouras, J., Jaskulek, S., et al. (2004). Magnetosphere imaging instrument (MIMI) on the Cassini mission to Saturn/Titan. In *The Cassini-Huygens Mission* (pp. 233–329). Springer. https://doi.org/10.1007/978-1-4020-2774-1_3

Lui, A. T. Y. (1996). Current disruption in the Earth's magnetosphere: Observations and models. *Journal of Geophysical Research*, *101*(A6), 13067–13088. https://doi.org/10.1029/96JA00079

Machida, S., Ieda, A., Mukai, T., Saito, Y., & Nishida, A. (2000). Statistical visualization of Earth's magnetotail during substorms by means of multidimensional superposed epoch analysis with Geotail data. *Journal of Geophysical Research*, *105*(A11), 25291–25303. https://doi.org/10.1029/2000JA900064

Masters, A. (2017). Model-based assessments of magnetic reconnection and Kelvin-Helmholtz instability at Jupiter's magnetopause. *Journal of Geophysical Research: Space Physics*, *122*, 11154–11174. https://doi.org/10.1002/2017JA024736

Partamies, N., Juusola, L., Whiter, D., & Kauristie, K. (2015). Substorm evolution of auroral structures. *Journal of Geophysical Research: Space Physics*, *120*, 5958–5972. https://doi.org/10.1002/2015JA021217

Slavin, J., Baker, D., Craven, J., Elphic, R., Fairfield, D., Frank, L., et al. (1989). CDAW 8 observations of plasmoid signatures in the geomagnetic tail. *An Assessment*, *94*(A11), 15153–15175. https://doi.org/10.1029/ja094ia11p15153

Slavin, J. A., Lepping, R. P., Gjerloev, J., Fairfield, D. H., Hesse, M., Owen, C. J., et al. (2003). Geotail observations of magnetic flux ropes in the plasma sheet. *Journal of Geophysical Research*, *108*(A1), 1015. https://doi.org/10.1029/2002JA009557

Vasyliunas, V. M. (1983). 11. Plasma distribution and flow. In *Physics of the Jovian magnetosphere* (pp. 395–453). Cambridge University Press. https://doi.org/10.1017/cbo9780511564574.013

Vogt, M. F., Jackman, C. M., Slavin, J. A., Bunce, E. J., Cowley, S. W. H., Kivelson, M. G., & Khurana, K. K. (2014). Structure and statistical properties of plasmoids in Jupiter's magnetotail. *Journal of Geophysical Research: Space Physics*, *119*, 821–843. https://doi.org/10.1002/2013JA019393

Vourlidas, A., Lynch, B. J., Howard, R. A., & Li, Y. (2012). How many CMEs have flux ropes? Deciphering the signatures of shocks, flux ropes, and prominences in coronagraph observations of CMEs. *Solar Physics*. https://doi.org/10.1007/s11207-012-0084-8

Yao, Z. H., Coates, A. J., Ray, L. C., Rae, I. J., Grodent, D., Jones, G. H., et al. (2017). Corotating magnetic reconnection site in Saturn's magnetosphere. *The Astrophysical Journal*, *846*(2), L25. https://doi.org/10.3847/2041-8213/aa88af

Young, D., Berthelier, J., Blanc, M., Burch, J., Coates, A., Goldstein, R., et al. (2004). Cassini Plasma Spectrometer Investigation. *The Cassini-Huygens Mission* (pp. 1–112).

Zong, Q. G., Fritz, T. A., Pu, T. A., Fu, Z. Y., Baker, D. N., Zhang, H., et al. (2004). Cluster observations of earthward flowing plasmoid in the tail. *Geophysical Research Letters*, *31*, L18803. https://doi.org/10.1029/2004GL020692

Erratum

An author's affiliations have been corrected. The present version may be considered the authoritative version of record.